Hybrid Modulation for Balancing Thermal Dissipation in Dual Active Bridge Converters

Liu, Bochen; Davari, Pooya; Blaabjerg, Frede

Published in:
2023 25th European Conference on Power Electronics and Applications (EPE'23 ECCE Europe)

DOI (link to publication from Publisher):
10.23919/EPE23ECCEEurope58414.2023.10264301

Publication date:
2023

Document Version
Accepted author manuscript, peer reviewed version

Hybrid Modulation for Balancing Thermal Dissipation in Dual Active Bridge Converters

Bochen Liu
Hitachi Energy
bochen.liu@hitachienergy.com

Pooya Davari
Aalborg University
pda@energy.aau.dk

Frede Blaabjerg
Aalborg University
fbl@energy.aau.dk

***Index Terms*—Thermal, DAB, Modulation, EPS**

***Abstract*—High thermal stress on the power semiconductor device is one of the main causes of the power electronics converter failures. Due to an imperfect design of the hardware circuit in practice and parameter variations in volume production, the problem of unbalanced thermal stress often appears on the power semiconductor devices. For addressing this issue, active thermal control is usually utilized to reduce the thermal loading of the most stressed power semiconductor device and thus improve the converter reliability. In dual active bridge (DAB) converters, the most often utilized modulation method is phase-shift PWM control. On this basis, it is possible to mitigate the thermal loading of the most stressed device by rerouting the current flowing path. In this letter, a hybrid modulation method is presented by combining the conventional extended-phase-shift (EPS) modulation and the proposed modified EPS modulation. A 1.5 kW converter prototype is established and comparative experimental results are shown to validate the effectiveness of the hybrid modulation to do thermal management.**

I. Introduction

THE failure mechanisms of power devices are mostly associated with the junction temperature swing and the high average junction temperature [1]. The former plays a more important role in the wear-out failures due to the nonconstant thermal expansion coefficients between different material layers, and the latter is more likely to cause catastrophic damage to the power device during transient or short-term operation [2, 3], especially when the ambient temperature of the working environment is very high, such as EVs [4]. For a given DAB converter, the reliability is usually limited by the most stressed power semiconductor device with the highest average junction temperature. One usual way to manage the thermal distribution is employing active thermal control methods [5], which are mostly obtained by means of rearranging the power losses distribution [6].

Since the first introduced single phase shift (SPS) modulation [7] for DAB converters can not achieve zero-voltage-switching (ZVS) over a wide power transfer range, especially when the input/output dc voltage ratio deviates far from 1 [8], many improved phase-shift modulation methods are proposed to extend the ZVS range, such as the extended-phase-shift (EPS) modulation [9], the dual-phase-shift (DPS) modulation [10] and the triple-phase-shift (TPS) modulation [11, 12]. The driving signals of all these improved methods are operating with a fixed 50 % duty cycle, indicating that the power devices have the same conduction time in one switching period.

However, thermal imbalance often occurs among the power semiconductor devices in practical situations, although all switches in a DAB converter have the same 50% duty cycle. In volume production of hardware components, the lot-to-lot parameter variations are unavoidable due to the manufacturing process shifts and drifts [13, 14]. For instance, despite under the same test conditions, there are usually minor variations of the on-state resistance for the same type of power semiconductor device, which can be reflected by the minimum value, typical value and maximum value in the data sheet. Besides, due to the various cooling system settings (e.g. the installation locations of the heatsinks and fans) in practical application environments, the heat dissipation ability (e.g. thermal resistance) from the junction to the ambient could vary. Another consequence is that the switches closer to the fans (or a heat source e.g. power supply) might have a higher (or lower) cooling efficiency compared to those not nearby. Both of them will further exacerbate the thermal imbalance. Moreover, the wear-out state of each power semiconductor device is not identical from a long-term perspective. One typical example is that a used power device has different electrical and thermal characteristics compared to the new one. Consequently, the junction temperatures of the power semiconductor devices in a DAB converter might differ from each other by considering the practical factors above.

In order to alleviate this thermal imbalance and reduce the thermal loading of the most stressed power semiconductor device, an EPS based hybrid modulation method by varying the duty cycles of corresponding switches is presented in this letter where firstly, the unbalanced thermal distribution using the conventional EPS modulation is described in Section II. Then the modified modulation method with adjustable duty cycles are introduced in Section III. Combining with the conventional EPS modulation, the principle and applying process of the proposed hybrid modulation method are also explained. Afterwards, four groups of experiments with different parameter configurations are conducted and the results are compared and discussed in Section IV. At the end, conclusions are summarized in Section V.

II. Unbalanced Thermal Distribution

The DAB circuit topology is shown in Fig. 1, consisting of two full bridges FB_1 and FB_2 on the primary and secondary sides of an isolated high-frequency transformer, respectively. Considering both the ZVS range extension and the applications where the DAB converter might most often operate in medium-load situations [12, 15], the extended-phase-shift (EPS) modulation type is studied in this paper. The working waveforms using conventional EPS modulation are shown in Fig. 2, where φ is the phase shift and α is the range of positive v_s. Thus, $\pi - \alpha$ will be the zero-voltage interval of v_s in a half switching period ($T_{sw}/2$). It can be seen that the driving

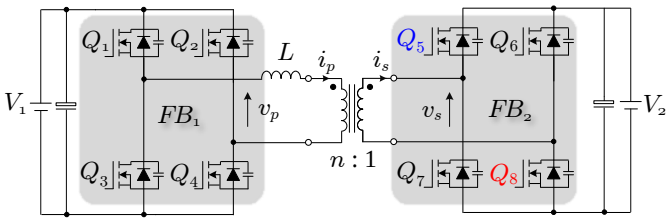

Fig. 1. Circuit topology of a DAB converter.

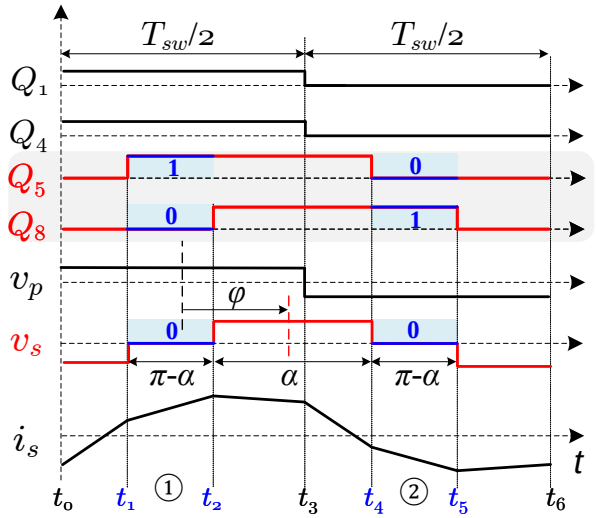

Fig. 2. Operating waveforms with conventional extended-phase-shift (EPS) modulation method (Conv. EPS).

signals for all power devices are with the same 50% duty cycle, where Q_1, Q_4, Q_5, Q_8 are as shown in Fig. 2 and the other four switches are complementary to them with a dead time to avoid short-circuit.

In order to observe the thermal imbalance in simulation, the practical factors (cf. Section I) causing unbalanced thermal dissipation are assumed equivalently leading to a different on-state resistance for Q_5 and Q_8, which are as $R_{ds,on,Q5} = 72\ m\Omega$ (typ. value from datasheet) and $R_{ds,on,Q8} = 80\ m\Omega$ (max. value from datasheet), respectively. The reason why Q_8 and Q_5 are selected is because Q_8 is found to be the most stressed power semiconductor device in the experiments, which will be presented in Section IV. Seen from the simulation results shown in Fig. 3, the junction temperatures $T_{j,Q8}$ and $T_{j,Q5}$ have a difference of $10°C$ when the converter reaches steady state at $t = 28\ ms$ using the conventional EPS modulation.

III. Proposed Hybrid Modulation Method

As presented in the last section, unbalanced thermal dissipation will result in different junction temperatures. In order to improve the reliability and lifetime of the DAB converter, the junction temperature of the most stressed power device should be reduced, without compromising other performances such as the power conversion efficiency. Considering that the conduction losses will dominate the total power losses if ZVS is achieved [8], the modified EPS modulation methods are firstly proposed to rearrange the conduction time of the power devices.

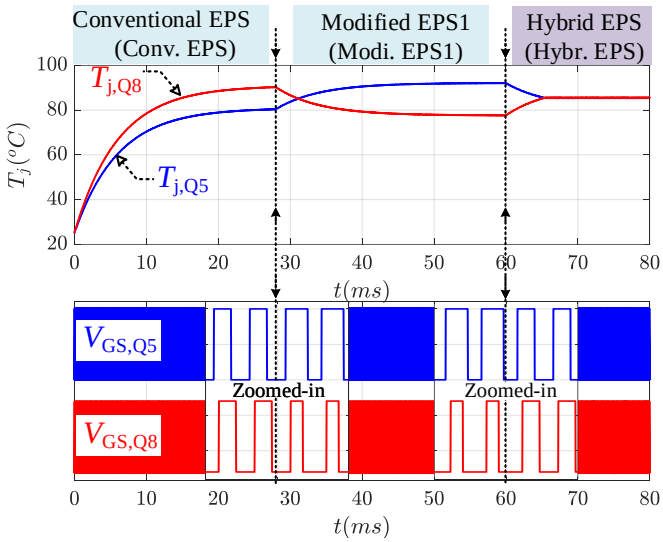

Fig. 3. Simulated junction temperatures of Q_5 and Q_8 using conventional, modified and hybrid EPS modulation methods with $R_{ds,on,Q5} = 22\ m\Omega$, $R_{ds,on,Q8} = 26\ m\Omega$ at $\alpha = 130°$, $\varphi = 60°$.

TABLE I
System Specifications for DAB Converter Prototype

Parameters	Description	Value
P	Rated power	1.5 kW
V_1	Input DC voltage	100 V
V_2	Output DC voltage	30 V
$n:1$	Turns ratio of the transformer	3.5 : 1
f_{sw}	Switching frequency	60 kHz
T_{dead}	Dead time	400 ns
L	Leakage inductance	45 μH

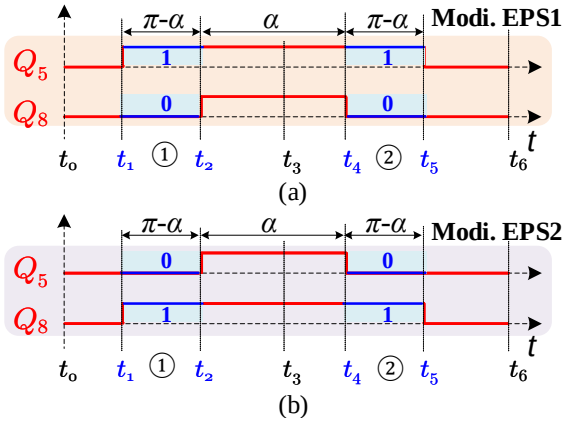

Fig. 4. Corresponding to the shaded area in Fig. 2, the proposed modified EPS to achieve (a) lower duty cycle for Q_8 - Modi. EPS1 (b) longer duty cycle for Q_8 - Modi. EPS2.

As shown in Fig. 2, zero-voltage intervals of v_s are provoked by turning on Q_5 and turning off Q_8 within $[t_1, t_2]$ (interval ①), and by turning off Q_5 and turning on Q_8 within $[t_4, t_5]$ (interval ②). In other words, the zero level of v_s can be generated by simultaneous turn-on Q_5, Q_6, or Q_7, Q_8 (cf. Fig. 1). If the turn-on and turn-off of a power device are respectively named by '1' and '0' as in Fig. 2, all possible combinations of the driving signals $V_{GS,Q5}$ and

TABLE II
CONVENTIONAL AND MODIFIED EXTENDED-PHASE-SHIFT (EPS) MODULATION METHODS

	Conv. EPS				Modi. EPS1		Modi. EPS2	
Fig. 2	①	②	①	②	①	②	①	②
$V_{GS,Q5}$	1	0	0	1	1	1	0	0
$V_{GS,Q8}$	0	1	1	0	0	0	1	1
D_{Q5}	0.5				$1-D_\alpha$		D_α	
D_{Q8}	0.5				D_α		$1-D_\alpha$	

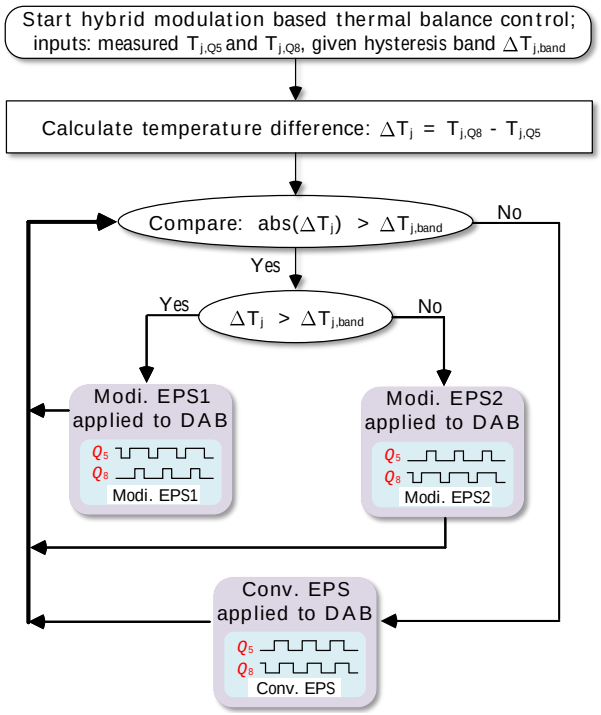

Fig. 5. Flow chart of the proposed hybrid modulation method for thermal balance.

$V_{GS,Q8}$ for achieving zero-level v_s are listed in Table II. Therein, $D_\alpha = \alpha/2\pi$ is used to represent the duty cycle of v_s.

In the conventional EPS modulation (Conv. EPS), the duty cycles of Q_5 and Q_8 are fixed at $D_{Q5} = 50\%$ and $D_{Q8} = 50\%$. Based on the practical requirements, the conduction time could be decreased or increased for Q_8/Q_7, corresponding to the modified EPS1 modulation (Modi. EPS1) and the modified EPS2 modulation (Modi. EPS2) in Fig. 4(a) and Fig. 4(b), respectively. It can be seen that the voltage shape of v_s is unchanged by replacing the driving signals of Q_5 and Q_8 in the conventional EPS (cf. Fig. 2) with the modified signals in Fig. 4.

Moreover, since the currents i_p and i_s (cf. Fig. 1) are determined by the voltage drop $v_p - nv_s$, which is maintained same in both Modi. EPS1 and Modi. EPS2, the leakage inductance current also can be maintained the same as the conventional EPS. This means that the modified EPS modulation in Fig. 4 will not change other converter performances such as the power conversion efficiency and the current stress of switches. The analysis and calculation of the power loss distribution for the built DAB setup can be found in [8].

In order to validate the effectiveness of the modified EPS modulation, Modi. EPS1 is applied to the DAB converter because $T_{j,Q8}$ is larger than $T_{j,Q5}$ using Conv. EPS, and the simulation result is shown within the range of $t \in [28\ ms, 60\ ms]$ in Fig. 3. It can be seen that the higher junction temperature of Q_8 starts decreasing at the beginning. However, a lower duty cycle of Q_8 also means a higher duty cycle of Q_5, and hence the thermal unbalance still exists with $T_{j,Q5} > T_{j,Q8}$ after the converter reaches steady state at $t = 60\ ms$.

To inhibit or even eliminate the thermal imbalances caused by only using the modulation method of Conv. EPS or Modi. EPS, the conventional and the modified EPS modulation methods are combined together to manage the thermal distribution of power devices. The flow cart of applying this hybrid modulation procedure is shown in Fig. 5. Firstly, the junction temperatures of $Q_1 \sim Q_8$ are obtained by direct measurement (e.g. thermal couple, optic fiber or infrared camera), or online calculation through an electro-thermal model [16, 17] or a junction temperature estimator [18]–[20]. Then the most stressed power device (i.e. Q_8 in this built DAB setup, cf. Section IV) can be confirmed by comparing the obtained junction temperatures. Afterwards, the corresponding modulation method is selected and applied to the DAB converter to reduce the high junction temperature of the most stressed power device. The selection rule is similar to the hysteresis control. If the maximum junction temperature error is within an acceptable range (i.e. the hysteresis band ΔT_j defined in Fig. 5), the conventional EPS is employed. Otherwise, Modi. EPS1 or Modi. EPS2 is implemented according to which power device has the highest junction temperature. Finally, DAB converter is continuously switched among the three modulation methods (i.e. Conv. EPS, Modi. EPS1 and Modi. EPS2) to reduce the duty cycle of the most stressed power device. Note that the value of ΔT_j is set at zero in the simulation. In practice, it can be set at other values considering the temperature measurement accuracy and the temperature adjustment ability. As shown in Fig. 3, $T_{j,Q5}$ and $T_{j,Q8}$ are coming much closer after using the proposed hybrid modulation method in the range of $t \in [60\ ms, 80\ ms]$, and the highest steady-state junction temperature is lower than only using Conv. EPS or Modi. EPS1.

IV. EXPERIMENT DESIGN AND DISCUSSION

In the built DAB setup, the secondary power semiconductor devices have a higher current than the primary side because of the $3.5:1$ turns ratio, and thus the experiments are focused on $Q_5 \sim Q_8$. Due to that the utilized discrete MOSFET structure for $Q_5 \sim Q_8$ (cf. Table I) has a package type of PG-TO220-3, it is difficult to directly measure the junction temperatures, and hence the case temperatures are measured instead. The measurement method in the experiments is to use a infrared camera focusing on the MOSFET case. As shown in Fig. 6, the individual heatsink for $Q_5 \sim Q_8$ is removed from the built DAB converter so that the infrared camera can have a clear view of the MOSFET case layer. In order to suppress the

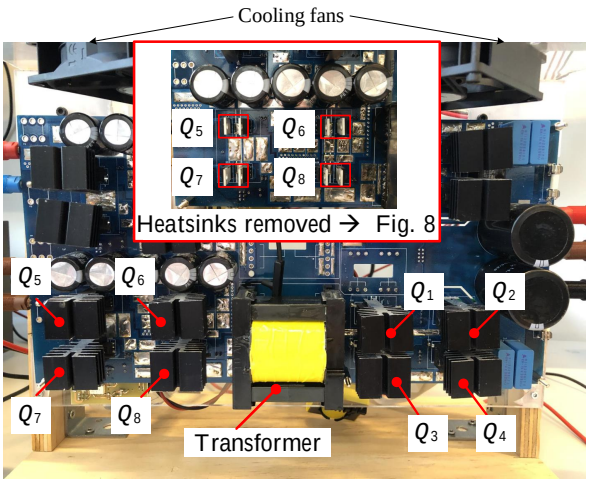

Fig. 6. Front view of the built DAB setup and amplified view of $Q_5 \sim Q_8$ with heatsinks removed in the top inset.

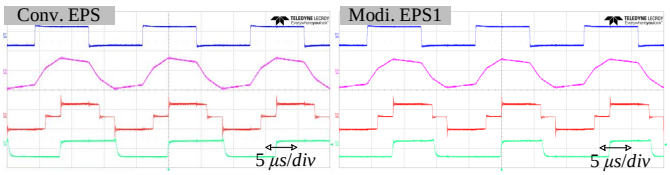

From top to bottom: v_p (200 *V/div*), i_s (35 *A/div*), v_s (50 *V/div*), $v_{GS,Q8}$ **(20 *V/div*)**

Fig. 7. Measured operating waveforms with Conv. EPS in the left inset and Modi. EPS1 in the right inset, both at $\alpha = 130°, \varphi = 60°$.

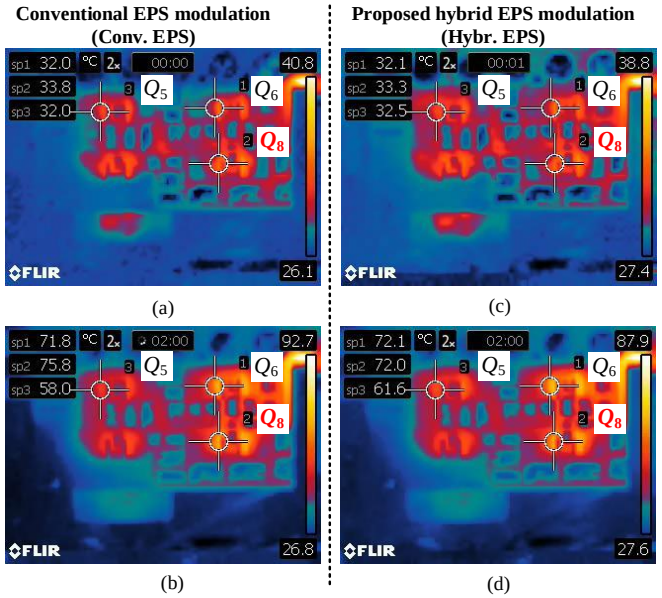

Fig. 8. Case temperature measurements by operating the DAB converter for 2 minutes with $\varphi = 60$ °: (a)/(b) initial/final temperatures using conventional EPS modulation method, (c)/(d) initial/final temperatures using the proposed hybrid EPS modulation method.

influence of reflectivity of other adjacent objects for a precise measurement, the PCB surface areas shown by the zoomed-in top inset in Fig. 6 are painted with black paint to increase the emissivity of MOSFET cases [21].

Besides, the fans for cooling down are also ceased during operation to avoid potential unbalanced heat dissipation for power devices $Q_5 \sim Q_8$, such as the uneven wind velocities between Q_5, Q_6 and Q_7, Q_8 in Fig. 6. As a result of heatsink removal and fans cease, the power devices $Q_5 \sim Q_8$ will be continuously heated up. It is necessary to operate the power devices within a safe temperature range and meanwhile to fairly compare the thermal effects of different modulation methods. Considering this, the continuous operation time for each experiment is set at 2 minutes to avoid overheat and the initial case temperatures are kept as identical as possible for each group of comparative experiments. The whole temperature changing process during the 2 minutes is recorded in a video. Accordingly, the initial and final case temperatures can be obtained by extracting the first and last frames from the video, respectively.

The steady state working waveforms with Conv. EPS and Modi. EPS1 are shown in Fig. 7. By operating the DAB converter with Conv. EPS for 2 minutes, the starting and ending case temperatures can be read from Fig. 8(a) and Fig. 8(b), respectively. It can be seen that the Q_8 (i.e. sp2 in Fig. 8) has the highest temperature increment of $42°C$ from the initial to the final state. As comparison, the proposed hybrid EPS (Hybr. EPS) modulation is applied by periodically operating the converter with a 12 seconds cycle loop of Conv. EPS for 8 seconds and then Modi. EPS1 for 4 seconds. In other words, the DAB converter is successively switched between Conv. EPS and Modi. EPS1 for 2 minutes. The initial and final measured results are illustrated in Fig. 8(c) and Fig. 8(d). Compared to Fig. 8(b), the final case temperature $T_{c,Q8}$ is reduced from $75.8°C$ to $72.0°C$ in Fig. 8(d). This means that the hybrid EPS modulation can effectively mitigate the thermal loading of the most stressed power device.

In order to comprehensively validate the effectiveness of thermal balancing method, another three groups of experiments (i.e. Group1, Group2 and Group3) with different phase-shift angles are conducted and the extracted initial and final $T_{j,Q8}$ are summarized in Table III. By comparing the case temperature increment $\Delta T_{c,Q8}$ for each group, the difference (Diff.) between the conventional (Conv.) and the proposed hybrid (Hybr.) EPS modulation are calculated and listed in the last column in Table III. It can be seen that the Hybr. EPS modulation leads to a lower temperature increment than the Conv. EPS modulation in all four groups of experiments. Therefore, the same conclusion can be achieved that utilizing the hybrid EPS modulation, it can effectively reduce the case temperature of the most stressed power device.

Furthermore, in order to verify whether the modified EPS modulation (i.e. Modi. EPS1 and Modi. EPS2 in Fig. 4) will impair the power conversion efficiency, the measured efficiencies under varied operating situations are listed in Table IV. It can be seen that the efficiencies are kept almost the same independent of the modulation method, which is consistent with the theoretical analysis in Section III.

V. Conclusions

In a DAB converter, there are multiple combinations of switching vectors to generate zero-level terminal voltage for a full-bridge. On this basis, a hybrid modulation method is proposed to mitigate the unbalanced thermal dissipation on power devices. By reconfiguring the switching sequence, the duty

TABLE III

SUMMARY OF THE MEASURED INITIAL AND FINAL CASE TEMPERATURES OF Q_8 WITH DIFFERENT CONTROL METHODS AND PHASE-SHIFT ANGLES

			$T_{c,Q8}$	$\boldsymbol{\Delta T_{c,Q8}}$	$\boldsymbol{Diff.}$
Group1	Conv. $\varphi = 35$ °	Initial	30.7^oC	$\mathbf{21.9^oC}$	$\mathbf{-1.3^oC}$
		Final	52.6^oC		
	Hybr. $\varphi = 35$ °	Initial	30.7^oC	$\mathbf{20.6^oC}$	
		Final	51.3^oC		
Group2	Conv. $\varphi = 45$ °	Initial	31.2^oC	$\mathbf{26.4^oC}$	$\mathbf{-3.2^oC}$
		Final	57.6^oC		
	Hybr. $\varphi = 45$ °	Initial	32.8^oC	$\mathbf{23.2^oC}$	
		Final	56.0^oC		
Group3	Conv. $\varphi = 55$ °	Initial	32.3^oC	$\mathbf{38.1^oC}$	$\mathbf{-4.8^oC}$
		Final	70.4^oC		
	Hybr. $\varphi = 55$ °	Initial	33.1^oC	$\mathbf{33.3^oC}$	
		Final	66.4^oC		
Group4	Conv. $\varphi = 60$ ° $\rightarrow$ Fig. 8(a)(b)	Initial	33.8^oC	$\mathbf{42.0^oC}$	$\mathbf{-3.3^oC}$
		Final	75.8^oC		
	Hybr. $\varphi = 60$ ° $\rightarrow$ Fig. 8(c)(d)	Initial	33.3^oC	$\mathbf{38.7^oC}$	
		Final	72.0^oC		

TABLE IV

MEASURED OPERATING EFFICIENCIES OF THE BUILT DAB CONVERTER WITH DIFFERENT MODULATION METHODS

Phase-shift	Conv. EPS	Modi. EPS1	Modi. EPS2
$\varphi = 35°$	93.4%	93.4%	93.4%
$\varphi = 45°$	92.8%	92.8%	92.8%
$\varphi = 55°$	91.4%	91.5%	91.4%
$\varphi = 60°$	90.6%	90.7%	90.7%

cycles of driving signals are varied instead of being fixed at 50%. The proposed hybrid modulation can be utilized to shift the thermal stress from the hottest device to relatively cooler devices without sacrificing other converter performances. e.g. efficiency.

Multiple groups of experiments with various operating parameters are conducted and the results prove that the proposed hybrid modulation can effectively alleviate the thermal imbalance. Note that the proposed hybrid method can also be applied to other modulation types (e.g. DPS, TPS) that contain zero-voltage levels in the full-bridge ac output.

REFERENCES

[1] H. Wang, M. Liserre, F. Blaabjerg, P. de Place Rimmen, J. B. Jacobsen, T. Kvisgaard, and J. Landkildehus, "Transitioning to physics-of-failure as a reliability driver in power electronics," *IEEE J. Emerg. Sel. Topics Power Electron.*, vol. 2, no. 1, pp. 97–114, 2014.

[2] S. Yang, A. Bryant, P. Mawby, D. Xiang, L. Ran, and P. Tavner, "An industry-based survey of reliability in power electronic converters," *IEEE Trans. Ind. Appl.*, vol. 47, no. 3, pp. 1441–1451, 2011.

[3] Z. Ni, X. Lyu, O. P. Yadav, B. N. Singh, S. Zheng, and D. Cao, "Overview of real-time lifetime prediction and extension for sic power converters," *IEEE Trans. Power Electron.*, vol. 35, no. 8, pp. 7765–7794, 2020.

[4] F. Blaabjerg, H. Wang, I. Vernica, B. Liu, and P. Davari, "Reliability of power electronic systems for EV/hev applications," *Proceedings of the IEEE*, pp. 1–17, 2021.

[5] M. Andresen, M. Liserre, and G. Buticchi, "Review of active thermal and lifetime control techniques for power electronic modules," in *Proc. 16th European Conf. Power Electronics and Applications*, 2014, pp. 1–10.

[6] J. Sheng, H. Yang, C. Li, M. Chen, W. Li, X. He, and X. Gu, "Active thermal control for hybrid modular multilevel converter under overmodulation operation," *IEEE Trans. Power Electron.*, vol. 35, no. 4, pp. 4242–4255, 2020.

[7] R. D. Doncker, D. Divan, and M. Kheraluwala, "A three-phase soft-switched high power density DC/DC converter for high power applications," in *Conference Record of the 1988 IEEE Industry Applications Society Annual Meeting*, IEEE, 1988.

[8] B. Liu, P. Davari, and F. Blaabjerg, "An optimized hybrid modulation scheme for reducing conduction losses in dual active bridge converters," *IEEE Journal of Emerging and Selected Topics in Power Electronics*, vol. 9, no. 1, pp. 921–936, 2021.

[9] B. Zhao, Q. Yu, and W. Sun, "Extended-phase-shift control of isolated bidirectional DC–dc converter for power distribution in microgrid," *IEEE Trans. Power Electron.*, vol. 27, no. 11, pp. 4667–4680, Nov. 2012.

[10] F. Li, Y. Li, and X. You, "Optimal dual-phase-shift control strategy of an isolated buck–boost converter with a clamped inductor," *IEEE Trans. Power Electron.*, vol. 33, no. 6, pp. 5374–5385, Jun. 2018.

[11] G. Xu, D. Sha, J. Zhang, and X. Liao, "Unified boundary trapezoidal modulation control utilizing fixed duty cycle compensation and magnetizing current design for dual active bridge DC–dc converter," *IEEE Trans. Power Electron.*, vol. 32, no. 3, pp. 2243–2252, Mar. 2017.

[12] A. Tong, L. Hang, G. Li, X. Jiang, and S. Gao, "Modeling and analysis of a dual-active-bridge-isolated bidirectional DC/dc converter to minimize RMS current with whole operating range," *IEEE Trans. Power Electron.*, vol. 33, no. 6, pp. 5302–5316, Jun. 2018.

[13] M. Pelstring. "Process shifts and drifts." (2017), [Online]. Available: https://www.durolabs.co/blog/2017/5/23/process-shifts-and-drifts.

[14] Z. Al Tarawneh, "The effects of process variations on performance and robustness of bulk cmos and soi implementations of c-elements," Ph.D. dissertation, Newcastle University, 2011.

[15] F. Krismer and J. W. Kolar, "Closed form solution for minimum conduction loss modulation of DAB converters," *IEEE Trans. Power Electron.*, vol. 27, no. 1, pp. 174–188, Jan. 2012.

[16] M. Chen, H. Wang, D. Pan, X. Wang, and F. Blaabjerg, "Thermal characterization of silicon carbide MOSFET module suitable for high-temperature computationally-efficient thermal-profile prediction," *IEEE J. Emerg. Sel. Topics Power Electron.*, p. 1, 2020.

[17] K. Ma, N. He, M. Liserre, and F. Blaabjerg, "Frequency-domain thermal modeling and characterization of power semiconductor devices," *IEEE Trans. Power Electron.*, vol. 31, no. 10, pp. 7183–7193, 2016.

[18] M. Andresen, M. Schloh, G. Buticchi, and M. Liserre, "Computational light junction temperature estimator for active thermal control," in *Proc. IEEE Energy Conversion Congress and Exposition (ECCE)*, 2016, pp. 1–7.

[19] N. Baker, M. Liserre, L. Dupont, and Y. Avenas, "Improved reliability of power modules: A review of online junction temperature measurement methods," *IEEE Ind. Electron. Mag.*, vol. 8, no. 3, pp. 17–27, 2014.

[20] H. Chen, B. Ji, V. Pickert, and W. Cao, "Real-time temperature estimation for power mosfets considering thermal aging effects," *IEEE Trans. Device Mat. Rel.*, vol. 14, no. 1, pp. 220–228, 2014.

[21] FLIR. "How does emissivity affect thermal imaging ?" (2019), [Online]. Available: https://www.flir.asia/discover/professional-tools/how-does-emissivity-affect-thermal-imaging/.